

# Learning What Matters: **P**rioritized **c**oncept Learning via **R**elative **E**rror-driven **S**ample **S**election

Shivam Chandhok<sup>\*1,2,4</sup>, Qian Yang<sup>\*1,3</sup>, Oscar Mañas<sup>1,3</sup>, Kanishk Jain<sup>1,3</sup>,  
Leonid Sigal<sup>†2,4,5</sup>, Aishwarya Agrawal<sup>†1,3,5</sup>

<sup>1</sup> Mila - Québec AI Institute <sup>2</sup> University of British Columbia

<sup>3</sup> Université de Montréal <sup>4</sup> Vector Institute for AI <sup>5</sup> Canada CIFAR AI Chair  
{qian.yang, aishwarya.agrawal}@mila.quebec {chshivam, lsigal}@cs.ubc.ca

## Abstract

Instruction tuning has been central to the success of recent vision-language models (VLMs), but it remains expensive—requiring large scale datasets, high-quality annotations and large-compute budget. We propose **P**rioritized **c**oncept learning **G** via **R**elative **E**rror-driven **S**ample **S**election – **PROGRESS** – a data- and compute-efficient framework that enables VLMs to dynamically select what to learn next based on their evolving needs during training. At each stage, the model tracks its learning progress across skills and selects the most *informative* samples: those it *has not already mastered* and *are not too difficult to learn* at the current state of training. This strategy effectively controls skill acquisition and the order in which skills are learned. Specifically, we sample from skills showing the highest learning progress, prioritizing those with the most rapid improvement. Unlike prior methods, PROGRESS requires no upfront answer annotations, querying answers only on a *need basis*, avoids reliance on additional supervision from auxiliary VLM, or compute-heavy gradient computations for data selection. Experiments across multiple instruction-tuning datasets of varying scales demonstrate that PROGRESS consistently outperforms state-of-the-art baselines with much less data and supervision. Additionally, we show strong cross-architecture generalization to different VLMs and transferability to larger models, validating PROGRESS as a scalable solution for efficient learning.<sup>2</sup>

## 1 Introduction

Multimodal vision-language models (VLMs) such as GPT-4V (OpenAI et al., 2024), Gemini (Team et al., 2023), LLaVA (Liu et al., 2023b,a), and InternVL (Chen et al., 2024b) demonstrate impressive general-purpose capabilities across tasks like image comprehension and visual question answering. Much of this success stems from large-scale fine-tuning on high-quality image-text corpora, particularly visual instruction-tuning (IT) datasets (Zhang et al., 2023; Xu et al., 2024), which significantly enhance instruction-following and reasoning abilities. A growing trend in building stronger VLMs has been to simply scale up: collecting larger more diverse IT datasets with better annotations and using them to instruction-tune increasingly powerful models (Chen et al., 2023; Liu et al., 2023a).

However, such pipelines are increasingly resource-intensive—annotation-heavy when relying on human-labeled supervision (*e.g.*, bounding boxes, object tags) and monetarily costly when generating instructions via proprietary models like GPT-4 (Liu et al., 2023b,a), alongside significant computational overhead. These factors make such pipelines increasingly inaccessible to individual

<sup>\*</sup>Equal Contribution, order determined by coin flip. <sup>†</sup>Equal Advising.

<sup>2</sup>Code will be released on publication.

researchers and smaller academic labs. More importantly, it is unclear whether the entirety of these large corpora is necessary for strong VLM performance. We posit that many samples are redundant or uninformative, and that comparable results could be achieved using fewer, informative samples.

To this end, we investigate how to select the *most informative* visual instruction-tuning (IT) samples based on the model’s own evolving learning state. We ask: *Can VLMs indicate what they can most effectively learn at a give stage of training?* Inspired by curriculum learning, we develop a framework in which the model periodically self-evaluates its current knowledge and identifies the skills it is ready to acquire next—those that would most benefit its learning progress. Specifically, we track the relative change in skill performance across iterations to estimate where learning improves fastest, encouraging the model to prioritize these skills. We hypothesize that this enables the VLM to actively select training samples that are most informative: those that are *not already mastered* by the model, and are *not too difficult* for the model to learn at its current stage. Overall, PROGRESS is designed to adapt to the model’s evolving learning state by helping it acquire essential skills, while also promoting diversity across selected concepts—a property crucial for capturing important modes in the data and supporting generalization.

Experimental results across multiple instruction-tuning datasets of varying scale demonstrate that PROGRESS achieves up to **99–100%** of the full-data performance while using only **16–20%** of the labeled training data. In addition to these gains, PROGRESS offers several practical advantages over existing approaches. First, unlike static scoring-based methods (Paul et al., 2021; Coleman et al., 2019; Marion et al., 2023; Hessel et al., 2022) or concept-driven strategies that rely on additional reference VLMs (Lee et al., 2024), our method uses dynamic feedback from the model’s own learning progress to guide training. Second, while many prior methods assume full access to ground-truth annotations upfront (Lee et al., 2024; Wu et al., 2025), we operate in a more realistic setting where the training pool is initially unlabeled and answers are queried only on a *need basis*—drastically reducing annotation cost. Third, instead of merely selecting *which* samples to train on (Lee et al., 2024; Wu et al., 2025), our approach also decides *when* to introduce each skill—enabling curriculum-style control over both skill acquisition and learning order. Our contributions are as follows:

- We propose **PROGRESS**, a dynamic, progress-driven framework for selecting the most informative samples during VLM instruction tuning—based on relative improvement across automatically discovered skills.
- Our method achieves near full-data performance using only 16–20% supervision across multiple instruction-tuning datasets of varying scale and across different VLMs—including the widely used LLaVA-v1.5-7B. It generalizes well across architectures, showing strong results on larger-capacity models like LLaVA-v1.5-13B and newer designs such as Qwen2-VL, while consistently outperforming competitive baselines and prior data-efficient methods.
- We analyze *what* skills the model prioritizes and *when*, revealing an interesting curriculum over skill types and difficulty—offering new insights into efficient VLM training.

## 2 Related Work

**Data Efficient Learning for VLMs.** Previous approaches for efficient VLM training (see Fig. 2) typically select a coreset—*i.e.*, a representative subset of the data—using static metrics like Clip-Score (Hessel et al., 2022) or score functions like EL2N (Paul et al., 2021), perplexity (Marion et al., 2023), entropy (Coleman et al., 2019), or train auxiliary scoring networks (Chen et al., 2024a). However, these methods perform one-time selection before training and fail to adapt to the model’s evolving needs. Score metrics often overlook important data modes, leading to poor diversity and reduced generalization (Lee et al., 2024; Maharana et al., 2025)—sometimes even underperforming random sampling (Lee et al., 2024). Other prominent work selects skill-diverse samples using reference VLMs—auxiliary models that themselves require large-scale instruction-tuning data to be effective. A notable example is COINCIDE (Lee et al., 2024), which clusters internal activations from a separately trained VLM model (*e.g.*, TinyLLaVA (Zhou et al., 2024)) for selection. This setup requires a fully trained additional VLM, ground-truth answers for full dataset, and manual human inspection to select appropriate activations for clustering—making it resource-intensive and hard to scale. Gradient-based methods (Wu et al., 2025; Liu et al., 2024b), while principled, are computationally prohibitive—requiring substantial memory to store high-dimensional gradients and

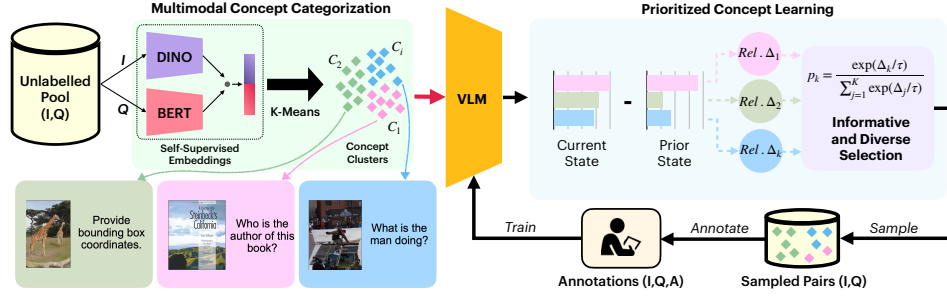


Figure 1: **Overall Pipeline.** Our framework consists of two stages: (1) *Multimodal Concept Categorization*, which partitions the unlabeled pool  $\mathbb{U}$  into distinct skills by assigning each sample  $(I, Q)$  to a specific skill cluster, and (2) *Prioritized Concept Learning*, where the model actively selects the most informative samples—those showing the highest improvement in its objective (e.g., accuracy or loss) relative to its prior state. Only these selected samples are annotated on a *need basis*, forming the labeled set  $(I, Q, A)$  and used for training.

large-scale compute (often upwards of 100 GPU hours, e.g., ICONS<sup>3</sup> (Wu et al., 2025))—directly refuting the goal of efficient training. Some methods also assume access to explicit knowledge of the target task or its distribution in the form of labeled samples—as in ICONS (Wu et al., 2025)—which is rarely available beforehand in practical settings for general-purpose VLM training.

**Curriculum Learning and Self-Paced Learning.** Curriculum learning improves generalization by presenting data from easy to hard (Bengio et al., 2009). Self-paced extensions adapt this ordering based on model own progress (Kumar et al., 2010; Sachan & Xing, 2016). These ideas have been explored in NLP (Sachan & Xing, 2016; Mindermann et al., 2022) as well as controlled synthetic multimodal settings (Misra et al., 2017) (e.g., CLEVR) on small-scale models, using external heuristics or limiting selection to question-level. In contrast, PROGRESS scales this principle to real-world instruction tuning of large VLMs by selecting informative image-text pairs at the skill level using unsupervised representations and dynamic learning progress signals.

**In summary**, our method brings together the best of all worlds (see Fig. 2): it selects and annotates samples dynamically adapting to the model’s learning state (*row 1*), effectively controlling skills and order of acquisition (*row 2*), require no additional reference VLMs for access to internal activations, no human-in-the-loop decisions (*row 3*), eliminates need for explicit knowledge of the target task or its distribution (*row 4*), or need for compute-heavy gradient computation (*row 5*), promotes diverse coverage of skills (*row 6*), —making it a practical solution for efficient and scalable VLM training. We apply supervision strictly on a *need basis* to only 20% of the dataset (*row 7*).

	Random	Perplexity	EL2N	Sem-DeDup	Self-Filter	ICONS*	COINCIDE	PROGRESS
1. Dynamic Selection	✗	✗	✗	✗	✗	✗	✗	✓
2. Order of Skills	✗	✗	✗	✗	✗	✗	✗	✓
3. Additional VLM Access	✗	✗	✓	✓	✓	✗	✓	✗
4. Target Task Access	✗	✗	✗	✗	✗	✓	✗	✗
5. Heavy-Gradient Overhead	✗	✗	✗	✗	✗	✓	✗	✗
6. Diversity	✓	✗	✗	✗	✗	✓	✓	✓
7. Answer Budget	20 %	20 %	100 %	100 %	100 %	100 %	100 %	20 %
8. Training Budget	20 %	20 %	20 %	20 %	20 %	20 %	20 %	20 %

Figure 2: **Comparison with Prior Efficient Learning Methods for VLMs.** **Green** denote **desirable** properties for efficient learning, while **Red** indicate **limitations**. PROGRESS *satisfies all key desirable criteria* while requiring only 20% data. See Appendix A for details of prior methods.

### 3 Problem Setting and Overall Framework

**Problem Setting.** We now formally introduce our data-efficient learning setting for training VLMs. We denote an image by  $I$ , a question by  $Q$ , forming an image-question pair  $(I, Q) \in \mathbb{U}$ , where  $\mathbb{U}$  is an unlabeled pool of such pairs. Unlike previous efficient learning methods, we do not assume access to the corresponding answers  $A \in \mathbb{A}$  for all pairs in  $\mathbb{U}$ , and thus refer to this pool as unlabeled. The learner is provided with: (1) the unlabeled pool  $\mathbb{U}$ ; and (2) a fixed answer budget  $b$ , specifying the maximum number of pairs from  $\mathbb{U}$  for which it can query an answer  $A \in \mathbb{A}$  and use for training, where  $|\mathbb{A}| = b \ll |\mathbb{U}|$ . The goal is to learn a vision-language model  $\text{VLM}(A \mid I, Q)$  that can accurately predict an answer for a new image-question pair, while only using  $b$  selected and labeled samples during training. The central challenge lies in identifying the *most informative*  $(I, Q)$  pairs

<sup>3</sup>Unpublished Concurrent work, we still reproduce and attempt to compare with it; see details in Appendix A.4.

to annotate within the constrained budget  $b$ , such that the resulting model trained on these  $(I, Q, A)$  pairs performs comparably to one trained on the fully labeled dataset.

**Overall Framework.** Our overall framework for efficient training of VLMs is shown in Figure 1. We employ a two-stage pipeline:

- (1) **Multimodal Concept Categorization.** Given an unlabeled data pool  $\mathbb{U}$  containing image-question pairs  $(I, Q) \in \mathbb{U}$ , we first partition  $\mathbb{U}$  into a distinct set of  $K$  skills, assigning each sample  $(I, Q)$  to a specific skill. This categorization enables tracking the model’s progress on individual skills and supports a self-paced training strategy where the model’s own learning signals determine which skills to prioritize next.
- (2) **Prioritized Concept Learning.** During training, the model periodically self-evaluates its knowledge by comparing its current performance to prior state, identifying skills where performance improves fastest relative to prior state. Samples  $(I, Q)$  from these skills are then selected and answer annotations  $A \in \mathbb{A}$  are queried only for these selected samples.

Overall, our model dynamically selects diverse, informative samples throughout training, in alignment with its evolving learning needs. To ensure that skill-level performance estimates are credible at the start of training—when the model is still untrained—we begin with a brief *warmup phase* (see details in Appendix A). This warmup, along with subsequent samples selected through our prioritized strategy, together make up the total annotation budget of  $b$ , ensuring that supervision in the form of  $(I, Q, A)$  **never exceeds the specified budget**. We validate that using the warmup set alone to train the model yields significantly worse performance compared to our proposed strategy—highlighting the importance of progress-driven sampling. Our framework allows the model to be trained with much less data and supervision, while controlling both skill acquisition and learning order.

### 3.1 Multimodal Concept Categorization

We begin by identifying diverse skills from the unlabeled data pool through a fully *unsupervised* concept categorization module that partitions  $\mathbb{U}$  into  $K$  skill clusters using spherical k-means. Each sample  $(I, Q) \in \mathbb{U}$  is assigned to a cluster based on cosine similarity from multimodal concatenated self-supervised DINO (Oquab et al., 2024) (for image  $I$ ) and BERT (Devlin et al., 2019) (for text question  $Q$ ) features. Jointly leveraging both modalities yields purer clusters with higher intra-cluster and lower inter-cluster similarity compared to unimodal partitioning (see Fig. 3)—enabling accurate tracking of skill-level progress during training. Unlike COINCIDE (closest best performing prior work) (Lee et al., 2024), our concept categorization framework is simpler, unsupervised, and more scalable. COINCIDE requires activations from fully trained additional VLM, ground-truth answers for full dataset, and human inspection to select appropriate activations for skill clustering. In contrast, our categorization is fully automated and practical, requires no labels, or manual introspection.

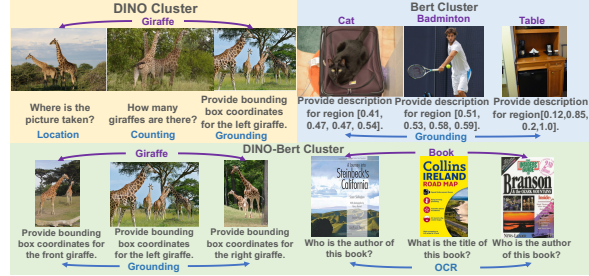


Figure 3: **Cluster Visualization.** Clustering with multi-modal DINO-BERT features ensures purer skill clusters with higher intra-cluster and lower inter-cluster similarity compared to uni-modal partitioning

### 3.2 Prioritized Concept Learning: Can VLMs indicate what they can most effectively learn at a give stage of training?

Our goal is to guide the VLM to prioritize skills it can most readily learn and improve upon. Since human intuition about task difficulty may not align with model’s difficulty in its feature and hypothesis space (Sachan & Xing, 2016), we adopt a self-paced strategy where the model’s own learning progress determines what to learn next. Inspired by curriculum learning (Kumar et al., 2010; Sachan & Xing, 2016), we select the most informative samples—those that yield the greatest improvement in the model’s objective (e.g., **accuracy or loss**) relative to its prior state.

Formally, given an unlabeled pool  $\mathbb{U} = \{(I, Q)\}$  partitioned into skill clusters  $\mathcal{C} = \{C_1, C_2, \dots, C_K\}$ , we define the model’s learning state at step  $t$  by its accuracy  $\text{Acc}_k^{(t)}$  on each clus-

ter  $k$ , computed over the training data seen by the model so far. The *relative change in performance* across steps quantifies learning progress per skill, which is then used to guide sample selection. We compute the expected accuracy improvement for each skill cluster between step  $t$  and  $t - \gamma$ :

$$\Delta_k = \frac{\text{Acc}_k^{(t)} - \text{Acc}_k^{(t-\gamma)}}{\text{Acc}_k^{(t-\gamma)} + \epsilon} \quad (1)$$

where  $\epsilon$  ensures numerical stability. The score  $\Delta_k$  captures how rapidly the model is improving on skill cluster  $k$ , serving as a proxy for sample *informativeness*. By prioritizing high  $\Delta_k$  clusters, the model focuses on skills it can improve on most rapidly—*thereby enforcing a self-paced curriculum* that dynamically adapts to the model’s learning state (Sachan & Xing, 2016)—controlling both the acquisition of skills and the order in which they are learned. In addition to the selection strategy in Eqn 1, we sample  $\delta\%$  of points at random to encourage exploration of new or underrepresented skills in dataset, following prior curriculum learning work (Kumar et al., 2010; Misra et al., 2017).

Only selected samples are annotated, forming the labeled set  $(I, Q, A)$  for training. This *need-based annotation* strategy avoids the costly requirement of full supervision used in prior coreset methods (such as COINCIDE (Lee et al., 2024)), offering a more scalable and efficient training paradigm.

However, naively selecting samples from only the highest-improvement cluster can hurt diversity by concentrating on a narrow skill set and leading to mode collapse—an issue known to degrade performance in prior work (Lee et al., 2024). To mitigate this, we propose to sample from multiple high  $\Delta_k$  clusters in proportion to their relative improvement using a *temperature-controlled softmax*:

$$p_k = \frac{\exp(\Delta_k/\tau)}{\sum_{j=1}^K \exp(\Delta_j/\tau)} \quad (2)$$

Here,  $p_k$  is the probability of sampling from cluster  $k$ , and  $\tau$  controls the sharpness of the distribution. Lower  $\tau$  emphasizes top clusters but risks mode collapse by repeatedly sampling from a narrow skill set (higher informativeness, lower diversity); higher  $\tau$  promotes broader sampling and better skill coverage. This balance between **informativeness and diversity** is critical for effective and robust learning (see ablation Fig. 4). The sampling budget at given step  $t$  is then allocated proportionally to  $p_k$ , and only the selected samples are annotated as  $(I, Q, A)$  triplets for training.

## 4 Experiments and Results

### 4.1 Experimental Setup

**Datasets and Models.** To demonstrate effectiveness and generalizability of our approach across different scales of instruction-tuning (IT) data, we conduct experiments on two IT datasets: Visual-Flan-191K (Xu et al., 2024) and the larger-scale LLaVA-665K (Liu et al., 2023b) containing  $\sim 0.6$  million samples. For the target VLMs, we use LLaVA-v1.5-7B (Liu et al., 2023b), following prior works. Additionally, we use LLaVA-v1.5-13B (Liu et al., 2023b) to test scalability and Qwen2-VL-7B (Wang et al., 2024) to test architecture generalization towards newer VLMs.

**Implementation Details.** Following standard protocol (Lee et al., 2024), we adopt LoRA (Hu et al., 2021) for training using the official hyperparameters from LLaVA-1.5. For the accuracy-based variant, we estimate cluster-wise accuracy using an LLM judge that compares the VLM output to ground-truth answers for samples in given cluster—though this is not required for our loss-based variant. Our setup follows standard evaluation protocols from prior work, ensuring consistency and fair comparison. Further details are provided in Appendix A.

**Baselines.** We compare PROGRESS against strong baselines spanning five major categories: (1) scoring function based methods (CLIP-Score, EL2N (Paul et al., 2021), Perplexity (Marion et al., 2023)); (2) deduplication-based selection (SemDeDup (Abbas et al., 2023)); (3) graph-based methods (D2-Pruning (Maharana et al., 2024)); (4) learned static selectors (Self-Filter (Chen et al., 2024a)); and (5) concept-diversity approaches (COINCIDE (Lee et al., 2024), Self-Sup (Sorscher et al., 2022)). We also include *Random*—a simple yet competitive baseline shown to perform well due to its diversity—and *Full-Finetune*, representing the performance upper bound with full supervision. Details for baselines follow previous work (Lee et al., 2024) and are provided in Appendix A.

**Evaluation Benchmark.** We evaluate our approach on a diverse suite of 14 vision-language benchmarks targeting different skills: perceptual reasoning (VQAv2 (Goyal et al., 2017), VizWiz (Gurari

Table 1: Comparison of coreset selection techniques for training LLaVA-v1.5 on the LLaVA-665K dataset using 20% sampling ratio. Methods highlighted in orange require additional reference VLMs and 100% dataset annotations for coreset selection, while methods highlighted in light green do not require either. The benchmark results are highlighted with best and second best models within the respective categories (i.e, with and without utilizing additional information). The best and the second best relative score are in **bold** and underlined, respectively.

Method	VQAv2	GQA	VizWiz	SQA-I	TextVQA	POPE	MME	MMBench	LLaVA-SEED	AI2D	ChartQA	CMMMU	Rel. (%)
								en	cn	Wild			
<b>LLaVA-v1.5-7B</b>													
0 Full-Finetune	79.1	63.0	47.8	68.4	58.2	86.4	1476.9	66.1	58.9	67.9	67.0	56.4	100
1 Self-Sup	74.9	59.5	46.0	67.8	49.3	83.5	1335.9	61.4	53.8	63.3	62.5	52.9	94.6
1 Self-Filter	73.7	58.3	<u>53.2</u>	61.4	52.9	83.8	1306.2	48.8	45.3	64.9	60.5	48.7	90.1
3 EL2N	76.2	58.7	43.7	65.5	53.0	84.3	1439.5	53.2	47.4	64.9	61.8	49.3	93.4
4 SemDeDup	74.2	54.5	46.9	65.8	55.5	84.7	1376.9	52.2	48.5	<u>70.0</u>	60.9	<u>53.5</u>	94.1
5 D2-Pruning	73.0	58.4	41.9	<u>69.3</u>	51.8	85.7	1391.2	<u>65.7</u>	<u>57.6</u>	63.9	62.1	52.5	94.8
6 COINCIDE	<u>76.5</u>	<u>59.8</u>	46.8	69.2	<u>55.6</u>	86.1	<u>1495.6</u>	63.1	54.5	67.3	<u>62.3</u>	53.3	97.8
7 Random	75.7	<u>58.9</u>	44.3	68.5	<u>55.3</u>	84.7	1483.0	62.2	54.8	65.0	61.7	50.2	95.0
8 CLIP-Score	73.4	51.4	43.0	65.0	54.7	85.3	1331.6	55.2	52.0	66.2	61.0	49.1	90.6
9 Perplexity	<u>75.8</u>	57.0	47.8	65.1	52.8	82.6	1341.4	52.0	45.8	<u>68.3</u>	60.8	48.7	91.1
<b>PROGRESS</b>													
10 Loss as Obj.	75.7	58.6	49.6	<u>70.1</u>	55.1	<u>86.3</u>	<u>1498.4</u>	<u>62.5</u>	<u>55.5</u>	65.5	<u>63.4</u>	<u>53.3</u>	98.4
11 Accuracy as Obj.	75.2	58.8	<u>53.4</u>	69.9	55.1	85.9	<u>1483.2</u>	61.1	54.4	65.5	<u>63.0</u>	<u>52.8</u>	<b>98.8</b>
<b>LLaVA-v1.5-13B</b>													
12 Full-Finetune	80.0	63.3	58.9	71.2	60.2	86.7	1541.7	68.5	61.5	69.5	68.3	60.1	100
13 Self-Sup	76.3	<u>60.5</u>	50.0	70.2	52.7	85.4	1463.8	63.7	57.6	64.9	65.2	53.3	93.8
14 Self-Filter	75.0	59.8	48.6	69.5	55.8	84.5	1446.9	58.8	51.8	<u>69.1</u>	65.3	52.4	92.6
15 EL2N	77.2	59.6	<u>54.8</u>	69.9	56.1	84.1	1531.0	59.3	52.3	65.8	<u>65.7</u>	<u>53.9</u>	94.4
16 SemDeDup	75.6	57.5	48.3	<u>70.5</u>	57.7	85.3	1397.6	59.0	51.1	68.7	64.9	53.2	92.9
17 D2-Pruning	73.9	<u>60.5</u>	49.8	70.4	55.2	84.9	1463.0	<u>67.3</u>	<u>59.9</u>	66.5	<u>65.9</u>	53.4	94.7
18 COINCIDE	<u>77.3</u>	59.6	49.6	69.2	<u>58.0</u>	87.1	<u>1533.5</u>	64.5	56.6	66.4	<u>65.9</u>	52.9	95.9
19 Random	76.7	<u>60.5</u>	48.0	68.8	57.7	84.8	1484.9	62.8	55.2	68.6	<u>65.5</u>	57.9	95.0
20 CLIP-Score	75.3	52.6	42.2	69.7	57.3	85.4	1426.3	60.4	54.0	68.1	63.3	52.8	91.8
21 Perplexity	<u>77.0</u>	58.5	48.2	68.7	54.8	83.1	<u>1508.8</u>	57.5	50.3	68.7	64.7	53.1	92.7
<b>PROGRESS</b>													
22 Loss as Obj.	76.8	59.7	<u>54.6</u>	70.4	<u>58.0</u>	87.2	1458.3	63.8	56.9	<u>69.9</u>	65.1	<u>58.0</u>	96.8
23 Accuracy as Obj.	76.9	58.9	53.0	70.1	57.5	87.1	1497.6	<u>63.9</u>	<u>57.6</u>	67.3	65.4	<u>57.7</u>	<u>96.5</u>

et al., 2018)), textual reasoning (TextVQA (Singh et al., 2019)), compositional reasoning (GQA (Hudson & Manning, 2019)), object hallucinations (POPE (Li et al., 2023b)), multilingual understanding (MMBench-cn (Liu et al., 2024a), CMMMU (Ge et al., 2024)), instruction-following (LLaVA-Bench (Liu et al., 2023b)), fine-grained skills (MME (Liang et al., 2024), MMBench-en (Liu et al., 2024a), SEED (Li et al., 2023a)), and scientific questions and diagrams (SQA-I (Lu et al., 2022), AI2D (Kembhavi et al., 2016), ChartQA (Masry et al., 2022)). See Appendix A for details.

**Evaluation Metrics.** We use standard evaluation metrics used by previous work to ensure consistency. Specifically, we use **average relative performance** Lee et al. (2024) to provide a unified measure for generalization. For each benchmark, relative performance is defined as:  $\text{Rel.} = \left( \frac{\text{Model Performance}}{\text{Full Finetuned Performance}} \right) \times 100\%$  This normalization allows us to normalize for the differences in the difficulty levels of different benchmarks following previous work.

## 4.2 Results and Analysis

**PROGRESS is more effective than existing SOTA in data efficient learning.** Table 1 (Row 0-11) compares PROGRESS against state-of-the-art baselines for training LLaVA-v1.5-7B on LLaVA-665K dataset under a 20% data budget, following standard settings.<sup>4</sup> PROGRESS achieves the highest relative performance (98.8%), outperforming all baselines, including those requiring access to ground-truth answers for the entire dataset and additional reference VLMs. In contrast, PROGRESS

<sup>4</sup>Reproduced with official code.



Table 2: **Architecture and Dataset Generalization.** For Architecture Generalization, we report Qwen2-VL-7B on the LLaVA-665K dataset using 20% sampling ratio. For Dataset Generalization, we report LLaVA-v1.5-7B on Vision-Flan dataset using 16.7% sampling ratio following prior work.

Method	VQAv2	GQA	VizWiz	SQA-I	TextVQA	POPE	MME	MMBench en	cn	LLaVA- Wild	SEED	Rel. (%)
Architecture Generalization (Qwen2-VL-7B)												
Full-Finetune	77.4	61.7	45.5	81.4	59.7	84.3	1567.9	76.1	75.1	84.8	66.9	100
Random	76.2	60.1	43.6	81.4	58.7	83.7	1556.8	76.8	74.5	81.7	67.6	98.7
COINCIDE	76.7	60.2	45.4	81.7	59.4	83.6	1583.5	77.4	76.2	80.5	67.9	99.6
PROGRESS	76.2	60.5	47.1	82.3	58.0	84.3	1560.1	77.2	72.9	87.1	67.6	100.0
Dataset Generalization (Vision-Flan-191K)												
Full-Finetune	69.4	46.0	49.7	59.9	34.1	85.1	1306.1	49.1	51.7	35.7	53.3	100
Random	66.0	43.8	52.2	62.1	39.7	82.7	1072.2	48.7	43.7	40.4	28.7	95.0
COINCIDE	66.3	43.6	51.0	63.8	35.2	81.9	1222.2	56.7	45.5	31.1	37.5	95.8
PROGRESS	65.5	44.0	53.6	62.5	42.0	82.9	1040.9	43.6	47.4	43.2	45.3	99.0

uses supervision only on a *need basis* for 20% of samples and relies solely on self-supervised features, yet reaching near-parity with full finetuning. PROGRESS also ranks among the top two methods on 8 out of 14 benchmarks, showing strong generalization across diverse tasks—e.g., including perception-focussed VQAv2 (75.2), scientific questions and diagrams (ChartQA:17.3, AI2D:52.8), and object hallucination POPE (85.9). Notably, it exceeds full-data performance on VizWiz (53.4 vs. 47.8), SQA-I (69.9 vs. 68.4), MME (1483.2 vs. 1476.9), ChartQA (17.3 vs. 16.4) and CMMM (24.6 vs. 22.1). These results demonstrate effectiveness the PROGRESS as a dynamic and fully automated alternative for efficient VLM training under limited supervision.

**Scalability to Larger Models.** To assess scalability, we use PROGRESS to train the larger LLaVA-v1.5-13B model under the same 20% data budget, testing whether our method developed for LLaVA-v1.5-7B transfers effectively to a higher-capacity model without hyperparameter tuning. As shown in Table 1 (Row 12-23), PROGRESS achieves a relative performance of 96.8%, outperforming all baselines. Beyond aggregate gains, PROGRESS ranks among the top-2 methods on 8 out of 14 benchmarks compared with all baselines, demonstrating strong generalization.

**Architectures and Dataset Generalization.** In Table 2, we test generalization of PROGRESS across different VLM architecture and IT dataset with accuracy as signal. For **architecture generalization**, we use newer Qwen2-VL-7B and train it on the LLaVA-665K dataset using the same 20% data budget and identical hyperparameters. We compare PROGRESS with two of the strongest (highest performing) established baselines—Random Sampling and COINCIDE—across multiple multimodal benchmarks. PROGRESS achieves the highest overall relative performance of 100% and ranks first or second on 9 out of 11 benchmarks (Tab. 2, **top**). For **dataset generalization**, we report LLaVA-v1.5-7B on Vision-Flan dataset under a stricter 16.7% annotation budget to assess generalization in low-resource settings. PROGRESS achieves the highest overall relative performance of 99.0%, outperforming COINCIDE (95.8%) and Random (95.0%) and ranks first or second on 8 out of 11 benchmarks (Tab. 2, **bottom**). The scalability and generalization are achieved without requiring any model-specific tuning. These results underscore the calability and generalization of PROGRESS , making it a practical solution for efficient training across diverse architecture and datasets.

### 4.3 Investigating the effectiveness of different components of PROGRESS

In this section, we provide further insights into the learning behaviour of PROGRESS . All experiments use LLaVA-v1.5-7B on the LLaVA-665K dataset with 20% sampling ratio and accuracy as the objective unless otherwise specified.

**How important is enforcing Diversity among the selected samples?** To assess the importance of balancing informativeness and diversity (Eqn 2), we conduct an ablation study varying the *temperature parameter*  $\tau$  in the softmax used for skill selection (Eqn 2). As

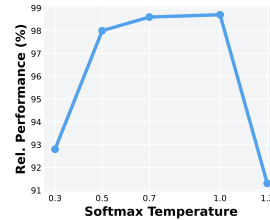


Figure 4: **Ablation of Softmax Temperature.** Both very-low and very-high temperatures lead to a significant performance drop.

Table 3: **Ablation of Selection Policy.** Performance comparison of different selection policies with the same warm-up strategy.

Method	VQAv2	GQA	VizWiz	SQA-I	TextVQA	POPE	MME	MMBench	LLaVA-	SEED	A12D	ChartQA	CMMMU	Rel. (%)	
								en	cn	Wild					
0 Full-Finetune	79.1	63.0	47.8	68.4	58.2	86.4	1476.9	66.1	58.9	67.9	67.0	56.4	16.4	22.1	100
1 Warm-up Only	73.1	55.9	43.8	67.9	54.2	85.4	1410.3	58.5	52.7	64.6	60.5	52.4	16.1	24.5	94.6
2 Random	75.7	59.0	43.8	68.8	54.9	85.6	1414.2	61.9	54.9	66.2	63.3	48.6	17.3	25.2	96.8
3 Easiest	72.0	54.8	50.2	67.1	51.6	85.7	1407.4	57.0	52.6	65.2	59.5	50.1	12.3	22.8	92.3
4 Medium	69.3	52.5	46.0	68.3	50.8	85.4	1307.6	54.6	48.7	62.5	57.7	47.6	14.3	26.1	91.1
5 Hardest	72.8	54.8	52.1	61.3	50.5	85.4	1364.8	37.9	34.5	67.5	54.1	41.4	15.8	25.9	88.5
PROGRESS															
6 Loss as Obj.	75.7	58.6	49.6	70.1	55.1	86.3	1498.4	62.5	55.5	65.5	63.4	53.3	17.3	23.7	98.4
7 Accuracy as Obj.	75.2	58.8	53.4	69.9	55.1	85.9	1483.2	61.1	54.4	65.5	63.0	52.8	17.3	24.6	98.8

shown in Figure 4, a *high temperature of 1.0* yields the **best overall performance** (98.8% relative score), striking an effective balance between prioritizing high-improvement clusters and maintaining diversity across concepts. As the temperature decreases (*i.e.*,  $\tau = 0.7, 0.5, 0.3$ ), performance consistently degrades, with the lowest temperature yielding only 92.8%—a significant drop of over 6% in relative score. This decline confirms that *overly sharp sampling distributions* (low  $\tau$ ) lead to *mode collapse*, where the model repeatedly focuses on a narrow set of concepts and fails to generalize broadly. Thus, we see that enforcing diversity helps improve performance. However, excessive diversity ( $\tau = 1.2$ ) is also not good as, in that case, the high-improvement clusters start losing their clear priority over other clusters.

**How effective is our Selection Policy?** We evaluate the efficacy of PROGRESS (sampling based on relative accuracy change - Sec 3.2) by comparing it against other competitive selection strategies: **Random Sampling**, **Easiest-Sampling** (selecting clusters with highest absolute accuracy at given time step), **Medium-Sampling** (selecting moderate accuracy clusters), and **Hardest-Sampling** (selecting lowest accuracy clusters). As shown in Tab. 3, PROGRESS achieves the highest relative score (98.8%), ranking first on 8 out of 14 benchmarks and second on 4 others. To further analyze learning dynamics across selection strategies, we categorize skill clusters into three difficulty levels—easy, moderate, and hard—based on their accuracy at the start of training. We then track the avg. performance of 50 clusters from each difficulty level for different selection strategies. As shown in Figure 5, PROGRESS consistently achieves higher mean performance and lower variance across all difficulty levels. These findings indicate that PROGRESS effectively balances learning across varying task difficulties, outperforming all other baseline strategies in both performance and stability.

#### How effective is PROGRESS under different sampling ratios?

We show relative performance on the Vision-FLAN dataset under different sampling ratios (even lower than 16.7 % considered in Tab. 2) in Figure 6. PROGRESS consistently outperforms

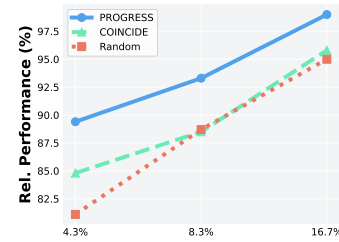


Figure 6: **Ablation of Sampling Ratio.** Relative performance on Vision-Flan dataset under different sampling ratio.

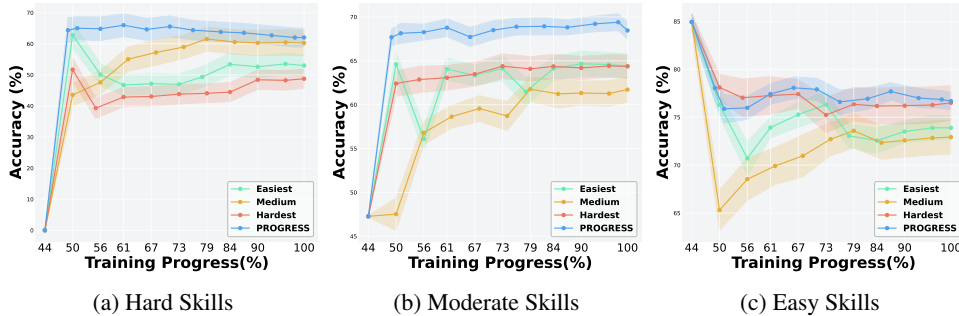


Figure 5: **Learning Dynamics Across Difficulty Levels.** PROGRESS consistently achieves higher accuracy and reduced variance compared to other selection strategies



strongest baselines - Random and COINCIDE across different sampling ratios, highlighting its effectiveness in prioritizing informative samples.

**How important is the order of skill acquisition?** Here we randomly shuffle PROGRESS-selected samples and perform training —thereby ablating importance of learning order. We find a 4.1% drop in relative performance, underscoring the importance of introducing appropriate skills at the right time. More details are in Appendix B.

**Wall Clock time** - More details in Appendix B.

#### 4.4 Digging Deeper into the Learning Behaviour of the Model

**How does the benchmark difficulty and data frequency impact performance?** Table 1 shows that PROGRESS enables efficient training. Here, we ask: *How does the degree of improvement correlate with factors such as benchmark difficulty and data frequency?* In Figure 7(a), we plot the accuracy improvement achieved by PROGRESS relative to warm-up-only model, as a function of benchmark difficulty. Difficulty is computed as the performance gap from full-data finetuning performance (*i.e.*,  $(100 - \text{full-finetune score})/100$ ), where a higher value indicates a more challenging benchmark (details in Appendix B). We find that PROGRESS yields the greatest performance gains on benchmarks of moderate difficulty. On the extremes, benchmarks like POPE (too easy) show limited gains as the model already performs well on them (has saturated), while harder benchmarks like ChartQA offer less benefit possibly due to difficult or rare skills being underrepresented in training data. To further investigate this, we plot accuracy improvement with respect to rarity in Figure 7(b), measuring for each benchmark the frequency of benchmark-aligned samples in training data and defining rarity as  $\log(1/\text{frequency})$  (see details in Appendix B). Once again, PROGRESS performs best in the mid-rarity range. Together, these results suggest a sweet spot of difficulty and frequency: easy skills show limited gains due to performance saturation, hard skills due to scarcity, and moderate skills benefit the most. This aligns with the Zone of Proximal Development (Vygotsky, 2012) and findings in (Khan et al., 2025), where learning is most effective just beyond current ability—neither too easy nor too difficult.

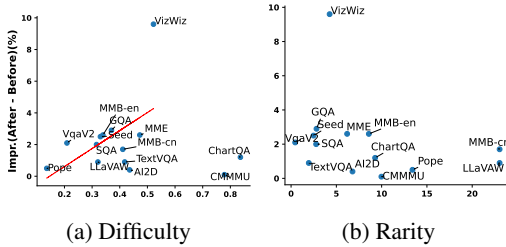


Figure 7: **Accuracy improvements** with (a) **benchmark difficulty** and (b) **sample rarity** in the training data. The largest performance gains occur in mid-range of difficulty and low-mid range of rarity.

Figure 8: **What skills model prioritize and when?** We analyze what skills are learned during the course of training (especially, in the beginning and towards the end). We use standard benchmark MME-defined (Liang et al., 2024) categories as it provides interpretable fine-grain abilities. Results are shown in Figure 8, panel (a) presents *grounded perceptual skills* - scene, position, and count, while panel (b) includes *language and symbolic skills* - OCR, text translation, and code reasoning. Each cluster is assigned a dominant ability (see Appendix B for the assignment algorithm). We track the number of samples selected per ability (shown as bars) and monitor corresponding accuracy trends throughout training on 20% samples. We observe that the model consistently performs better on certain abilities than others. For example, scene recognition outperforms position understanding, and OCR yields higher accuracy than both text translation and code reasoning. Interestingly, as shown in Fig. 8(a), the model initially prioritizes *count* (at iteration 541), but accuracy does not improve — likely because it is too early in training to benefit from learning this skill. The model temporarily shifts focus and improves other abilities (*i.e scene*), then revisits *count* and *position* abilities at iteration 738, where accuracy now increases and later stabilizes. In Fig. 8(b), *OCR* initially shows a decline in accuracy, but the model gradually selects more OCR-relevant samples. At iteration 738, it selects the most OCR samples, leading to the largest accuracy gain. Toward the end of training, the model increasingly focuses on more difficult abilities like *code reasoning* and *text translation*, with sample selection and performance rising after iteration 790. Notably, PROGRESS outperforms full-data fine-tuning performance (denoted by dashed line) on these challenging skills, despite using only 20% of data.

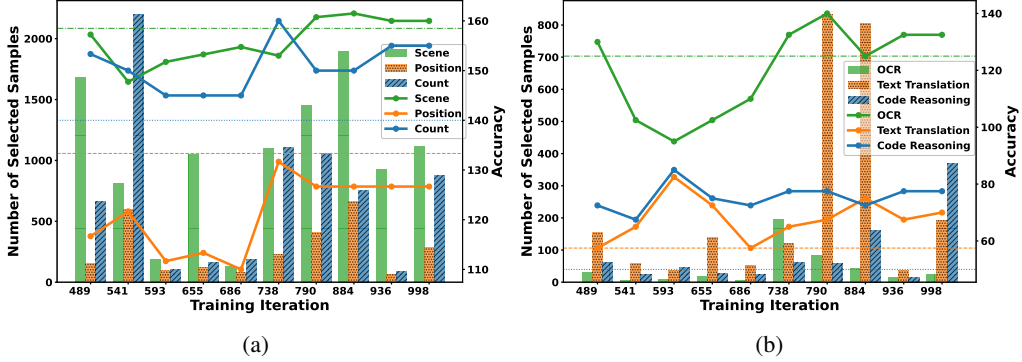


Figure 8: **What skills model prioritize and when?** We track the number of samples selected per ability (shown as bars) and monitor corresponding accuracy trends throughout training on 20% samples. The dashed horizontal lines show full-data fine-tuning performance for comparison.

## 5 Conclusion

We introduce PROGRESS, a dynamic and data-efficient framework for instruction-tuning VLMs under a strict data and supervision budget. By tracking learning progress across unsupervised skill clusters and prioritizing samples that are most learnable at each stage, PROGRESS effectively controls both the acquisition and order of skills. Our method achieves near full-data performance with just 16–20% supervision while requiring no additional reference VLMs, requires annotations only on *need basis*, and scales across architectures and datasets. Extensive experiments show that this self-paced, progress-driven strategy outperforms strong baselines while offering practical advantages in scalability, diversity, and data efficiency.

## 6 Limitations

While PROGRESS effectively orders and prioritizes more informative skills, it randomly samples within each selected skill cluster without ranking samples by usefulness. Additionally, the accuracy-based variant incurs extra inference time to compute skill-level progress (see Appendix A), though our loss-based variant avoids this issue. However, overall, PROGRESS outperforms prior approaches while requiring no additional reference VLM and significantly less supervised data.

## Acknowledgments

We acknowledge the valuable feedback provided by Aditya Chinchure, Le Zhang, Shravan Nayak, and Rabiul Awal on the early draft. The technical support extended by the Mila IDT team in managing the computational infrastructure is greatly appreciated. Additionally, Aishwarya Agrawal and Leonid Sigal received support from the Canada CIFAR AI Chair award throughout this project.

# Appendix

In this appendix section, we provide additional details that could not be included in the main paper due to space constraints:

- Additional details on the **Baselines** used, including setup and implementation (extending Sec.4.1 and Fig. 2 of the main manuscript).
- **Implementation** details and **hyperparameter** settings (extending Sec.4.1).
- Comparison with concurrent work ICONS (extending Sec.4.2 and Sec 2).
- Further Ablation studies on the **Effect of Hyperparameters** and **Wall-clock Time** comparisons (extending Sec.4.3).
- **Word Cloud Visualization** for our multimodal clustering approach (extending Sec.3.1).
- Visualization of the **Diversity** of samples selected by our method (extending Sec. 4.3).
- Additional details on the setup and algorithms used for our analysis (extending Sec.4.4).

## A Details of Experimental Setups

### A.1 Baselines

We follow the standard experimental settings and implementation protocols for all baselines as established in recent prior work (see COINCIDE (Lee et al., 2024)), using official code. For completeness, clarity and reproducibility, we additionally provide detailed descriptions of each baseline here.

**COINCIDE** (Lee et al., 2024) is a strong coreset selection method that leverages concept-based clustering and mutual transferability between clusters to guide sample selection. It performs coreset selection only once before training by clustering internal activations of a separately trained additional reference VLM (e.g., TinyLLaVA(Zhou et al., 2024)). It relies on static selection strategy that does not adapt to the model’s learning progress, requires an additional pretrained VLM, ground-truth annotations for full dataset to extract activation maps, and manual intervention to select appropriate activation layers—making the method resource-intensive and difficult to scale.

**CLIP-Score** (Hessel et al., 2022) It ranks image-instruction pairs based on visual-textual similarity computed by the CLIP model (Radford et al., 2021), selecting top-scoring samples for training. While this approach assumes that higher similarity indicates greater informativeness, it relies on static, precomputed metrics that do not adapt to the model’s learning progress. Prior work (Lee et al., 2024) has shown that such metrics often fail to capture important data modes, resulting in reduced diversity and suboptimal generalization—limitations that PROGRESS overcomes through dynamic, progress-driven selection.

**EL2N** (Paul et al., 2021) ranks training samples based on the expected L2-norm of prediction error:  $\mathbb{E}[\|p(x) - y\|_2]$  where  $p(x)$  is the token distribution predicted by a reference VLM,  $x$  is the input, and  $y$  is the ground-truth label. This score reflects how confidently and accurately the reference model predicts each sample. However, it requires access to a fully trained additional VLM and ground-truth labels for the entire dataset, making it resource-intensive and static.

**Perplexity** (Marion et al., 2023) measures the uncertainty in the model’s predictions and is defined as  $\exp(-\mathbb{E}[\log p(x)])$ , where  $p(x)$  denotes the likelihood assigned to input  $x$  by a additional reference VLM model. Samples from the middle of the perplexity distribution are selected, following prior work (Lee et al., 2024). However, it requires access to a fully trained additional VLM and, like other static metrics, often fails to capture important data modes—potentially limiting diversity and downstream generalization.

**SemDeDup** (Abbas et al., 2023) aims to reduce redundancy by removing semantically duplicated samples. It clusters the output embeddings of the final token from a reference model’s last layer and retains a diverse subset by eliminating near-duplicates and reducing redundancy. This method also

requires an additional reference VLM to extract the final token features and ground-truth labels for the entire dataset.

**D2-Pruning** (Maharana et al., 2024) constructs a graph over training data where nodes encode sample difficulty and edges capture pairwise similarity. It selects a diverse coreset by pruning this graph while preserving representative and challenging samples. Difficulty is measured using the AUM score, defined as  $p_y(x) - \max_{i \neq y} p_i(x)$ , where  $p_y(x)$  is the model’s confidence for the ground-truth label  $y$ . Similarity is computed using the L2 distance between average final-layer token embeddings from an additional reference VLM. This method requires access to an additional reference VLM for embedding extraction and scoring and ground-truth labels for the entire dataset.

**Self-Sup** (Sorscher et al., 2022) clusters data using averaged output embeddings from the final-layer tokens of a reference model. It assigns scores based on distance to cluster centroids, selecting samples that are closest—assumed to be the most prototypical representatives of the data distribution. This method also requires access to an additional reference VLM for embedding extraction.

**Self-Filter** (Chen et al., 2024a) is a recent coreset selection method originally proposed for the LLaVA-158k dataset (containing three vision-language tasks). It jointly fine-tunes a scoring network alongside the target VLM on the *entire labeled dataset*, using this as learned reference model to score and filter training samples—hence it requires an additional reference model trained on full data with full annotations. Following previous work (Lee et al., 2024), we adopt the stronger variant that also incorporates CLIP scores and features.

**Random.** We additionally report results for *Random*, which finetunes the model using a coreset selected via random sampling. Despite its simplicity, Random serves as a strong and competitive baseline—prior work (Lee et al., 2024) has shown that random sampling often preserves sample diversity and can outperform more complex selection methods in certain settings.

*Note:* We use standard setup for the baseline implementations as described prior work (see COINCIDE Appendix). For **COINCIDE**, **EL2N**, **SemDeDup**, **D2-Pruning**, and **Self-Sup**, we use image, question, and ground-truth answer for full dataset as inputs along with additional reference VLM (i.e TinyLLaVA) to extract features following prior work (Lee et al., 2024). **Self-Filter** requires full dataset to finetune additional reference network—the score-net. As a result, these baselines require an additional reference vision-language model or full dataset annotations (100%) or both.

## A.2 Implementation Details.

In this section, we provide elaborate details on implementation of our approach in continuation to the brief details we provide in Section 4.1 of main manuscript.

We first partition the unlabeled data pool  $\mathcal{U}$  into  $K$  skill clusters using spherical k-means, following the fully *unsupervised* concept categorization procedure described in Section 3.1. Training begins with a brief warmup phase (see details in Appendix A.3), which equips the model with basic instruction-following capability and ensures that skill-level performance estimates are reliable in the beginning of training.

Subsequently, we apply our Prioritized Concept Learning (PCL) strategy (see Section 3.2) to estimate the expected performance improvement for each skill cluster between iteration  $t$  and  $t - \gamma$  (as defined in Eqn 1), using either accuracy or loss as the tracking metric (see Table 1, row 10 and 11). For the accuracy-based variant, we compute

Table 4: Hyperparameter configurations.  $K$  represents the number of clusters.

Method	LLaVA-1.5	Vision-Flan
CLIP-Score	high score selected	high score selected
EL2N	medium score selected	medium score selected
Perplexity	medium score selected	medium score selected
SemDeDup	$K : 10,000$	$K : 5,000$
D2-Pruning	$k : 5, \gamma_r : 0.4, \gamma_f : 1.0$	$k : 5, \gamma_r : 0.4, \gamma_f : 1.0$
Self-Sup	$K : 10,000$	$K : 5,000$
Self-Filter	$k : 10, \gamma : 1$	$k : 10, \gamma : 1$
COINCIDE	$K : 10,000, \tau : 0.1$	$K : 5,000, \tau : 0.1$
<b>PROGRESS</b>		
<b>Warmup Stage</b>		
Number of Clusters	$K : 10,000$	$K : 5,000$
Warmup Ratio (w.r.t full data)	9%	8.4%
<b>Prioritized Concept Learning</b>		
Number of Clusters	$K : 1,000$	$K : 200$
Temperature of Softmax	$\tau : 1.0$	$\tau : 1.0$
BatchSize	128	128
Selection Gap	$\gamma * \text{BatchSize} : 7,500$	$\gamma * \text{BatchSize} : 3,500$
Random Exploration	$\delta\% : 10\%$	$\delta\% : 10\%$

cluster-wise accuracy using an LLM judge as metric that compares the VLM output to ground-truth answers—though this is not required for our loss-based variant. Samples are then selected using a temperature-controlled softmax over the improvement scores (see Eqn 2). This selection process is repeated every  $\gamma$  iterations, and in each round, we sample a total of  $\gamma * BatchSize$  examples for annotation and training. We refer to this  $\gamma * BatchSize$  as selection gap from here on.

**Hyperparameters for Baselines and PROGRESS** To ensure fair comparison, we use the same hyperparameters as COINCIDE (Lee et al., 2024) for all baselines. The hyperparameters for both the baselines and PROGRESS are summarized in Table 4. For model training, we apply LoRA (Hu et al., 2021) to LLaVA-v1.5 and follow the official fine-tuning settings provided in the LLaVA-1.5 release. For Qwen2-VL, we perform full fine-tuning using the official hyperparameters specified by Qwen2-VL. For accuracy estimation, we use LLMs such as InternLM2-Chat-20B (Cai & et al., 2024) as the judge. We provide the question, ground-truth answer, and predicted answer (without the image) as input and ask the LLM to decide whether the prediction is correct. The full prompt is shown below in Table A.2. Ablation studies on all hyperparameters are provided in Section 4.3 and Appendix B.

#### Prompt for Accuracy Estimation

Given an input question and two answers: a candidate answer and a reference answer, determine if the candidate answer is correct or incorrect.

**Rules:**

- The candidate answer is correct if it is semantically equivalent to the reference answer, even if they are phrased differently.
- The candidate answer should be marked as incorrect if it:
  - Contains factual errors compared to the reference answer
  - Only partially answers the question
  - Includes hedging language (e.g., "probably", "likely", "I think", etc.)
  - Answers a different question than what was asked
- Give a reason for your prediction.

**Output Format:**

- Answer - correct or incorrect
- Reason -

### A.3 Warmup Phase

Following prior work (Xia et al., 2024; Wu et al., 2025), we begin with a brief warmup phase using a small subset—9% of the total dataset pool size (see ablation in Fig. 9 (a))—to equip the model with basic instruction-following capability and ensure that skill-level performance estimates are credible at the start of training—when the model is still untrained. These early estimates are crucial for tracking relative learning progress across skills in subsequent training phases.

To be effective, the warmup set should provide broad skill coverage across diverse clusters and include transferable examples that support generalization to unseen skills that model will later learn. To this end, we adopt the sampling strategy from Lee et al. (2024), selecting samples from each cluster proportionally to:  $P_i \propto \exp(S_i/\tau D_i)$  where  $S_i$  denotes the cluster’s *transferability* and  $D_i$  its *density*. This prioritizes clusters that are both diverse and likely to generalize well, ensuring a representative warmup set.

Importantly, the entire warmup set selection used for our method utilizes clusters generated using concatenated DINO and BERT derived features (as explained in Sec. 3.1)—instead of requiring additional reference VLMs features or ground-truth answers. As shown in Appendix B, we validate that training solely on this warmup set (without our Prioritized concept learning module in Section 3.2) yields significantly worse performance compared to our proposed strategy—highlighting the importance of our progress-driven sampling.

Table 5: Statistics of ICONS target validation sets.

Dataset	MME	POPE	SQA-I	MMB-en	MMB-cn	VQAv2	GQA	VizWiz	TextVQA	LLaVA-W
$ \mathcal{D}_{val} $	986	500	424	1,164	1,164	1,000	398	8,000	84	84
$ \mathcal{D}_{test} $	2,374	8,910	4,241	1,784	1,784	36,807	12,578	8,000	5,000	84

Table 6: Comparison between PROGRESS and ICONS. Repro. means reproductions of ICONS.

Method	VQAv2	GQA	VizWiz	SQA-I	TextVQA	POPE	MME	MMBench en cn Wild	LLaVA- SEED AI2D ChartQA CMMMU	Rel. (%)
0 Full-Finetune	79.1	63.0	47.8	68.4	58.2	86.4	1476.9	66.1 58.9	67.9 67.0 56.4 16.4 22.1	100
1 ICONS	76.3	60.7	50.1	70.8	55.6	87.5	1485.7	63.1 55.8	66.1 - - - -	-
2 ICONS (Repro.)	75.0	57.7	45.9	63.7	55.1	86.0	1434.0	47.1 37.3	68.4 57.3 45.3 17.2 24.3	91.6
<b>PROGRESS</b>										
3 Loss as Obj.	75.7	58.6	49.6	70.1	55.1	86.3	1498.4	62.5 55.5	65.5 63.4 53.3 17.3 23.7	98.4
4 Accuracy as Obj.	75.2	58.8	53.4	69.9	55.1	85.9	1483.2	61.1 54.4	65.5 63.0 52.8 17.3 24.6	98.8

#### A.4 Comparison with ICONS

**ICONS** (Wu et al., 2025) is a concurrent unpublished work that differs significantly from our approach. It requires **(1)** high memory and compute resources—reportedly over 100 GPU hours—to compute and store gradient-based influence scores for selection, and **(2)** access to explicit knowledge of the target task or its distribution in the form of labeled samples from validation set of target benchmarks. This assumption is impractical in general-purpose VLM training, where target tasks may be unknown at training time and usage of such high-compute refutes the goal of efficient learning. As such, **ICONS is not directly comparable** and falls outside the scope of our setting, which avoids both gradient-based selection and downstream task knowledge from target benchmarks prior to training the VLM model.

Nevertheless, we strive to compare with them in good faith by reproducing ICONS using their official codebase for fair comparison. Although ICONS has released its codebase, the validation data (for each target benchmark) it uses to simulate target task knowledge is not publicly available. The paper reports the number of validation samples used per benchmark (see Table 5), however the specific validation samples remain unspecified and are not publicly released. To approximate their setup, we randomly select an equal number of samples from the publicly available validation sets of target benchmarks and reproduce their performance.

Table 6 presents results across three settings: Row 1 shows the original ICONS results as reported; Row 2 presents our reproduction using their codebase and randomly selected validation samples; Rows 3 and 4 report results for PROGRESS. We observe that PROGRESS outperforms our ICONS reproduction in relative performance even though our method does not rely on compute-intensive gradient-based selection and does not assume any knowledge from target benchmarks, reinforcing the practicality and effectiveness of our method under realistic constraints.

## B Further Ablation Studies and Analysis

### B.1 Ablation Studies

**Ablations on Hyperparameter** We conduct further ablations studies in Fig. 9 on effect of hyperparameters. All experiments use LLaVA-v1.5-7B on the LLaVA-665K dataset with 20% sampling ratio and accuracy as the objective. Fig. 9(a) shows the effect of different warm-up ratios relative to the total training data pool size. Our results show that a 9% warm-up ratio achieves the best performance, as it strikes a balance between preparing the model adequately and leaving enough room for our iterative Prioritized concept learning strategy to select informative samples. The 20% warm-up ratio (i.e using only warmup selected samples to entirely train the model eliminating our Prioritized concept learning strategy completely), results in significantly reduced performance in overall relative score. Next, Fig. 9(b) shows the effect of varying the number of clusters  $K$  used for our concept categorization module (Section 3.1). Using too few skill-clusters reduces skill diversity and leads to lower purity (in terms of skill types) within given cluster, while too many clusters result in redundant clusters of the same skill category and insufficient samples per cluster to yield credible



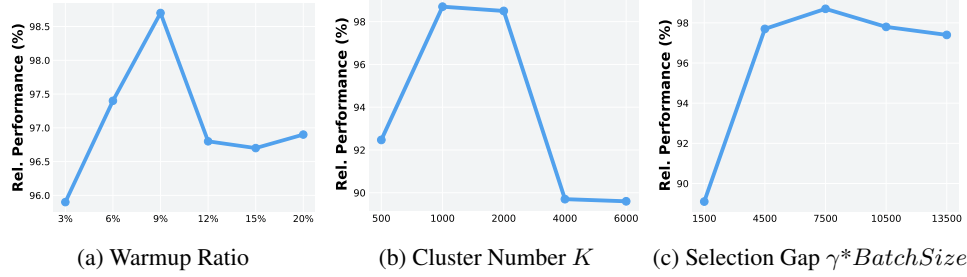


Figure 9: **Ablation Studies.** (a) Effect of the warm-up ratio. (b) Effect of the number of clusters. (c) Effect of the selection gap.

accuracy estimates. We find that using approximately 1,000-2000 clusters strikes the best balance and yields optimal performance. Finally, Fig. 9(c) shows the influence of the selection gap i.e  $\gamma * BatchSize$  (see definition in Appendix A.2). We find that the model is particularly sensitive to small gaps; for instance, a gap size of 1,500 leads to a rapid performance decrease. Smaller gaps cause the model to switch too soon, not allowing it to learn the selected concepts sufficiently.

**How important is the order of skill acquisition?** Unlike prior methods that focus solely on selecting which samples to use (Lee et al., 2024; Wu et al., 2025), PROGRESS also controls when to introduce them during training (Section 3.2)—effectively guiding both skill selection and the order of acquisition. To assess the importance of learning order, we ablate this component by randomly shuffling the data selected by PROGRESS and training the model without respecting the intended sequence. Even with the same data, training in a random order leads to a noticeable performance drop—from 98.8% to 94.6%—highlighting that when to introduce concepts is just as important as what to learn.

**Wall-clock Time Comparison.** We present wall-clock time analysis with Qwen2-VL-7B on the LLaVA-1.5 dataset using 20% selected data for training. We compare average relative performance (Rel.) against wall-clock time for two of the highest-performing baselines—COINCIDE (Lee et al., 2024) and Random. PROGRESS (Accuracy as Objective) achieves relative performances of 96.3%, 97.1%, 98.2%, 99.1%, and 100% with wall-clock times of 1.5, 1.75, 2.5, 4, and 5.67 hours, respectively—making PROGRESS Pareto superior to COINCIDE. Full fine-tuning on entire dataset (with 100% data) takes about 9 hours. Note that the plot includes only actual data selection and model training time for both methods and excludes the time to train additional reference VLM model which COINCIDE needs for clustering and also accuracy estimation inference time for cluster accuracy evaluation using an LLM judge for our method. For our approach, accuracy estimation using LLM overhead is minimal when leveraging online concurrent APIs—and can be further reduced by using loss as the objective variant of our method which provides state-of-art performance and does not require cluster level accuracy estimation (see performance in Table 1 in main manuscript).

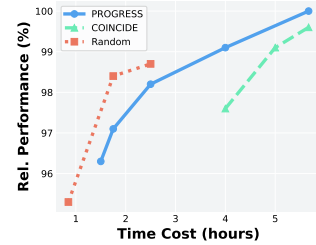


Figure 10: **Wall-clock time comparison.** The time cost is measured in hours of running time on a computing node with  $4 \times A100$  GPUs.

## B.2 Details for Analysis in main manuscript- How does the benchmark difficulty and data frequency impact performance?

In this section, we elaborate on details regarding the analysis in Section 4.4, where we analyze the impact of benchmark difficulty and data frequency.

### B.2.1 Details for Benchmark Difficulty Analysis

Here, we provide details regarding the analysis shown in Fig. 7 (a) of main manuscript.

---

**Algorithm 1** Sample Rarity Estimation via Gaussian Modeling

---

**Require:** Training dataset  $\mathbb{U} = \{x_1, \dots, x_N\}$  where  $x_i = (I_i, Q_i)$ ; set of benchmarks  $\mathcal{B} = \{B_1, \dots, B_M\}$  with  $M$  different benchmarks.

- 1: **Feature Extraction:** Extract DINO features from images and BERT features from questions; concatenate to form joint feature vectors, for all training and benchmark samples.  
We denote DINO-BERT embedding of  $x_i$  as  $\phi(x_i)$
- 2: **Fit Gaussian Models:** Fit multivariate Gaussian  $\mathcal{N}(\mu_j, \Sigma_j)$  for each benchmark  $B_j$  using its feature vectors
- 3:  $n_j \leftarrow 0, \forall j \in \{1, \dots, M\}$  {Initialize match counts for each benchmark}
- 4: **for** each training sample  $x_i \in \mathbb{U}$  **do**
- 5:    $\ell_j = \log \mathcal{N}(\phi(x_i) \mid \mu_j, \Sigma_j), \forall j \in \{1, \dots, M\}$  {Log-likelihoods under each benchmark’s Gaussian}
- 6:    $k = \arg \max_j \ell_j$  {Assign to benchmark with highest likelihood}
- 7:    $n_k \leftarrow n_k + 1$  {Increment matched sample count for  $B_k$ }
- 8: **end for**
- 9: **for** each benchmark  $B_j \in \mathcal{B}$  **do**
- 10:    $f_j = n_j / N$  {Compute frequency}
- 11:    $r_j = \log(1/f_j)$  {Compute rarity}
- 12: **end for**
- 13: **return**  $\{r_1, \dots, r_M\}$  {Rarity scores for all benchmarks}

---

**Quantifying Benchmark Difficulty.** Prior work has shown that human intuition about task difficulty may not align with a model’s difficulty as defined in its feature or hypothesis space (Sachan & Xing, 2016). Therefore, we use the model’s own performance as a proxy for determining benchmark difficulty. Specifically, we use the performance of full-dataset fine-tuned LLaVA-v1.5-7B (i.e., Row 0 in Table 1) as reference to determine difficulty of benchmark—benchmarks with higher performance are considered easier. We define **benchmark difficulty** for a given benchmark as  $(100 - \text{Performance of full fine-tuned LLaVA-1.5 on Benchmark})/100$ . This gives us a difficulty measure for each benchmark normalized between  $[0, 1]$ <sup>5</sup>.

**Quantifying Performance Improvement.** To isolate the impact of our core contribution—Prioritized Concept Learning (PCL) described in Section 3.2—we measure the performance improvement brought solely by our dynamic sample selection strategy. Specifically, we compute the difference in performance between the full PROGRESS framework (Table 3, Row 7) and the warm-up only model trained prior to applying PCL (Table 3, Row 1). This comparison quantifies the gain attributable to dynamically selecting the most informative samples using our PCL strategy during training.

## B.2.2 Details for Data frequency Analysis

Here, we provide details regarding the analysis shown in Figure 7 (b) of main manuscript.

**Sample Rarity Estimation.** Our goal is to identify, for each sample in the training dataset, the benchmark it most closely aligns with in terms of skill distribution. Each training sample is assigned to exactly one benchmark—whichever it is closest to—based on similarity in distribution over skills. This allows us to estimate the frequency of training samples aligned with each benchmark, enabling us to quantify how commonly each benchmark’s skills are represented in the training data.

**Assignment Procedure.** To quantify how training samples align with various benchmarks, we use a Gaussian modeling approach. Specifically, we first extract visual and textual features using DINO (for images) and BERT (for questions) and form joint multimodal embeddings as described in Section 3.1—for all samples in training data and each benchmark.

Next, we fit a multivariate Gaussian distribution to each benchmark’s embeddings, capturing its mean and covariance to model the underlying skill distribution. Then, for every training sample, we

---

<sup>5</sup>For MME, where the full score is not out of 100, we normalize the score by dividing it by the maximum score (2800), the difficulty is computed as  $(1 - \text{MME Score}/2800)$

---

**Algorithm 2** Ability Assignment for Clusters

---

**Require:** Training dataset  $\mathbb{U} = \{x_1, \dots, x_N\}$  where  $x_i = (I_i, Q_i)$ ; Clusters  $\mathcal{C} = \{C_1, \dots, C_K\}$ ; samples from MME benchmark  $\mathcal{B} = \{b_1, \dots, b_M\}$  with ability labels; similarity threshold  $\alpha = 0.9$ ; top- $k$  nearest neighbors ( $k = 5$ )

- 1: **Feature Extraction:** Extract DINO features for images and BERT features for questions; concatenate to form joint feature vectors, for all training and benchmark samples. We denote DINO-BERT embedding of  $x_i$  as  $\phi(x_i)$ .
- 2: **for** each cluster  $C_k \in \mathcal{C}$  **do**
- 3:   **for** each sample  $x_i \in C_k$  **do**
- 4:      $\mathcal{N}_i = \{\text{TopK}(\text{sim}(\phi(x_i), \phi(b_j)))_{j=1}^M\}$  where  $\text{sim}(\phi(x_i), \phi(b_j)) = \cos(\phi(x_i), \phi(b_j))$
- 5:      $\mathcal{N}'_i = \{b_j \in \mathcal{N}_i \mid \text{sim}(\phi(x_i), \phi(b_j)) \geq \alpha \cdot \max_j \text{sim}(\phi(x_i), \phi(b_j))\}$
- 6:      $\mathcal{A}_i = \{\text{ability}(b_j) \mid b_j \in \mathcal{N}'_i\}$
- 7:   **end for**
- 8:    $\mathcal{A}_k = \bigcup_{x_i \in C_k} \mathcal{A}_i$  {Aggregate ability labels from all samples in  $C_k$ }
- 9:    $\text{Ability}(C_k) = \text{Mode}(\mathcal{A}_k)$  {Assign the most frequent ability via majority vote}
- 10: **end for**
- 11: **return**  $\{\text{Ability}(C_1), \dots, \text{Ability}(C_K)\}$

---

compute the log-likelihood under each benchmark’s Gaussian model, reflecting how well the sample fits that benchmark’s distribution. Each training sample is then assigned to the benchmark with the highest log-likelihood (refer to Algorithm 1 for full details).

We compute the frequency of training data samples aligned with each benchmark as the proportion of training samples assigned to it:

$$\text{frequency} = \frac{\# \text{ matched samples}}{\text{total training samples}}.$$

Finally, we define the rarity as:

$$\text{rarity} = \log(1/\text{frequency}).$$

This formulation enables us to assess how frequently the skills associated with each benchmark appear in the training set (see rarity calculation Algorithm 1).

### B.3 Details for Analysis - What Skills Does the Model Prioritize and When?

In this section, we elaborate on the analysis from Section 4.4 (specifically Fig. 8 in main manuscript), where we investigate which skills the model prioritizes and when during training.

Our goal is to identify the specific ability each skill-cluster—obtained through our concept categorization module described in Section 3.1—represents and track both the number of selected samples and the performance of that skill over time. To do this, we assign each skill cluster in our framework to one of the standardized ability categories defined by the MME benchmark (i.e *count*, *position*, *OCR* etc) which offer interpretable and fine-grained labels covering both perception and cognitive tasks. To determine the dominant ability for each skill-cluster, we use a similarity-based assignment procedure (see Algorithm 2 for details).

We first extract visual and textual features using DINO (for images) and BERT (for questions) and form joint multimodal embeddings as described in Section 3.1—for all samples in training data and MME benchmark dataset.

For each training sample in a given skill-cluster generated by our concept categorization module, we compute its cosine similarity with all samples in the MME benchmark. We identify its top- $K$  nearest neighbors in MME benchmark and retain only those with similarity above a 90% threshold, ensuring that we capture the most aligned MME samples for each training example. MME abilities associated with these filtered neighbors are aggregated for samples in the cluster, and majority voting is applied to assign the most frequent ability to the entire cluster. This process offers a principled way to characterize each skill-cluster’s dominant visual-linguistic ability, ensuring robustness through both similarity filtering and voting (refer to Algorithm 2 for more details).

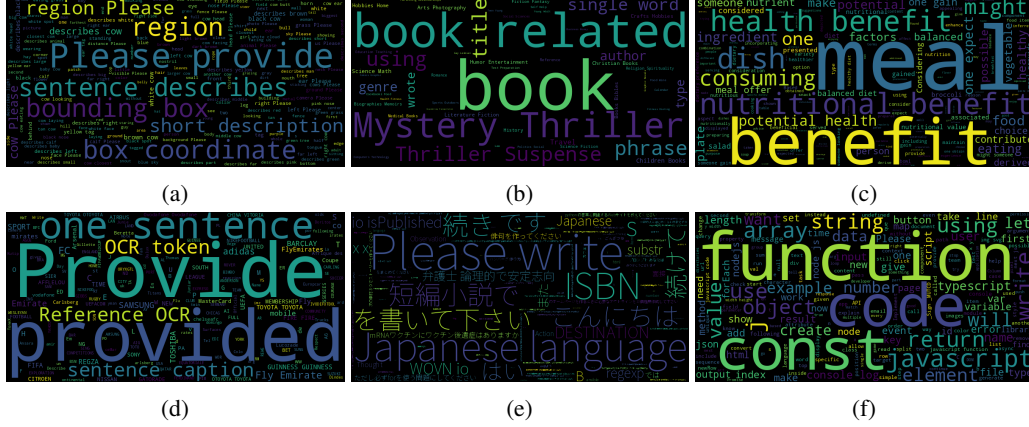


Figure 11: **Word Cloud Visualization of Skill Clusters.** Each subfigure shows the word cloud generated by concatenating all questions within a single skill-cluster discovered by our unsupervised concept categorization module. The clusters exhibit clear semantic themes: (a) object localization and region descriptions, (b) book metadata and genres, (c) food and nutritional benefits, (d) OCR, (e) multilingual Japanese text and language prompts, and (f) programming and function-related instructions. These word clouds highlight the semantic coherence and fine-grained granularity of the automatically discovered clusters, validating their utility for skill-level progress tracking.

## C Analysis

### C.1 Word Cloud Visualization of Skill Clusters

To qualitatively assess the semantic coherence and purity of discovered skill clusters obtained through our concept categorization module (Section 3.1), we generate word clouds by aggregating all questions from all samples assigned to a given cluster. For each cluster, we concatenate all the corresponding questions into a single string and visualize the most frequent words using wordclouds. Note that we remove standard stopwords while plotting the wordclouds.

Figure 11 shows representative word clouds for six clusters. Each cluster exhibits a distinct semantic theme, validating the purity and fine-grained granularity of the automatically discovered clusters and demonstrating the effectiveness of our multimodal concept categorization. For example, cluster (a) object localization and region descriptions, (b) book metadata and genres, (c) pertains to food and nutritional benefits, (d) corresponds to OCR and reference tokens, (e) involves multilingual Japanese text and language prompts, and (f) highlights programming and function-related tasks.

These visualizations demonstrate that our clustering method forms fine-grained, interpretable concept groupings while being fully unsupervised (see Section 3.1)—essential for skill-level tracking and prioritized learning in PROGRESS.

### C.2 Skill-level Diversity in Selected Sample Distribution

To better understand the selection behavior across methods, we follow protocol in previous work (Lee et al., 2024) and analyze the number of selected samples from each task in the Vision-Flan-191K dataset. Figure 12 shows the task-wise sample distribution for PROGRESS and several baseline approaches.

We observe that methods relying on single static scoring functions—such as CLIP-Score, EL2N, Perplexity, and Self-Sup—tend to exhibit strong sampling bias, disproportionately selecting from a small subset of tasks while neglecting others. This narrow focus often overlooks important data modes, leading to poor generalization—a limitation also noted in prior work (Lee et al., 2024).

In contrast, PROGRESS maintains a more balanced and diverse sampling profile across tasks, ensuring that a broader range of skills and task types are represented during training. This diversity stems from our skill-driven selection strategy, which tracks learning progress across clusters and samples proportionally using a temperature-controlled distribution.

Overall, by avoiding the pitfalls of static scoring and overfitting to specific high-scoring skills or frequent tasks, our method instead promotes broader and more effective skill acquisition.

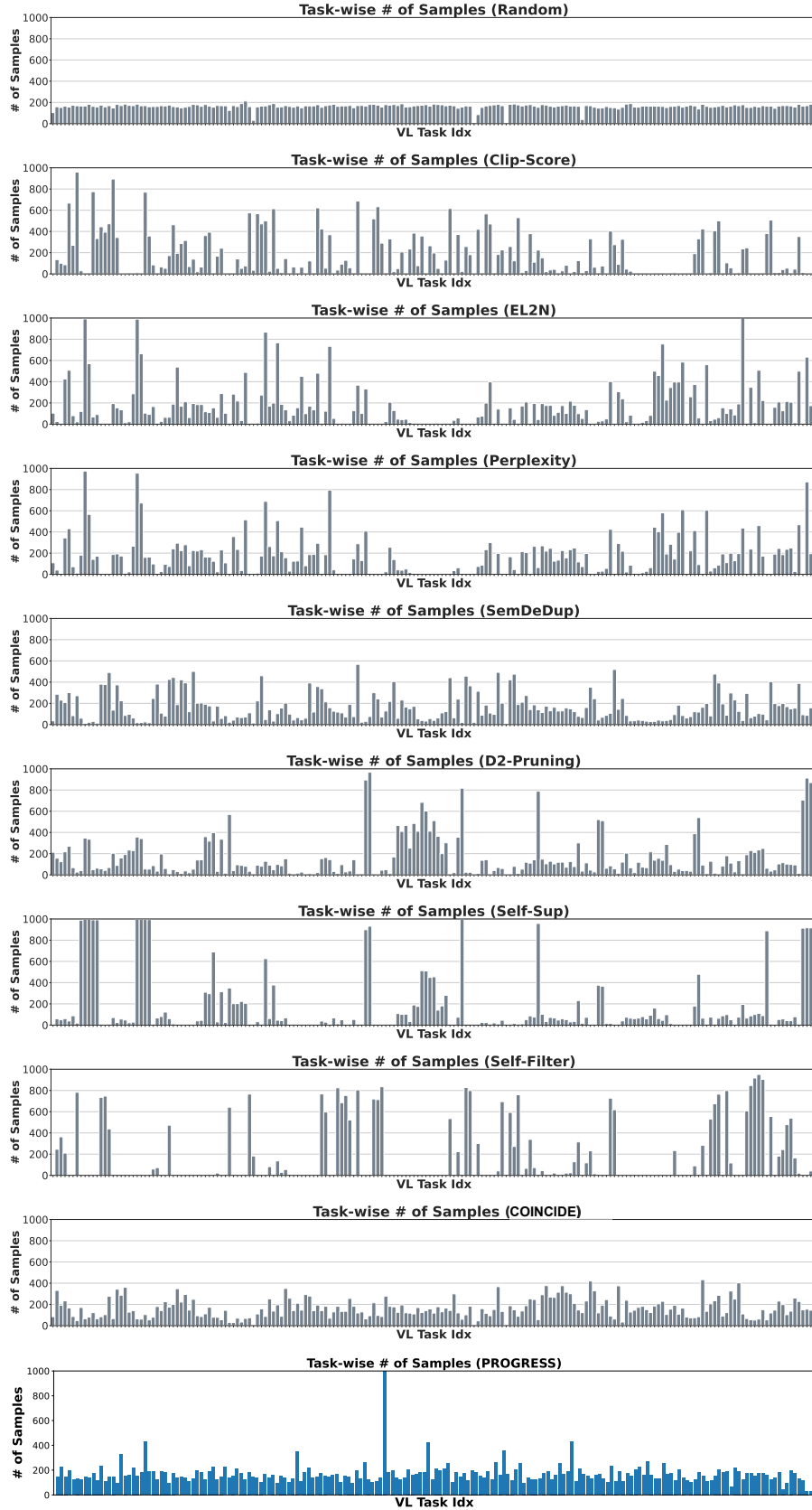


Figure 12: **Task-wise Distribution of Selected Samples.** Number of samples selected (y-axis) from each Vision-Flan-191K task (x-axis) across different methods. While baselines tend to concentrate heavily on a few high-scoring tasks, PROGRESS achieves a more balanced sampling pattern across the task spectrum—highlighting its ability to maintain skill diversity.

## References

- Amro Kamal Mohamed Abbas, Kushal Tirumala, Daniel Simig, Surya Ganguli, and Ari S Morcos. Semdedup: Data-efficient learning at web-scale through semantic deduplication. In *ICLR 2023 Workshop on Mathematical and Empirical Understanding of Foundation Models*, 2023.
- Yoshua Bengio, Jérôme Louradour, Ronan Collobert, and Jason Weston. Curriculum learning. In *Proceedings of the 26th annual international conference on machine learning*, pp. 41–48, 2009.
- Zheng Cai and et al. Internlm2 technical report, 2024.
- Lin Chen, Jisong Li, Xiaoyi Dong, Pan Zhang, Conghui He, Jiaqi Wang, Feng Zhao, and Dahua Lin. Sharegpt4v: Improving large multi-modal models with better captions. *arXiv preprint arXiv:2311.12793*, 2023.
- Ruibo Chen, Yihan Wu, Lichang Chen, Guodong Liu, Qi He, Tianyi Xiong, Chenxi Liu, Junfeng Guo, and Heng Huang. Your vision-language model itself is a strong filter: Towards high-quality instruction tuning with data selection. In *Findings of the Association for Computational Linguistics ACL 2024*, pp. 4156–4172, 2024a.
- Zhe Chen, Jiannan Wu, Wenhai Wang, Weijie Su, Guo Chen, Sen Xing, Muyan Zhong, Qinglong Zhang, Xizhou Zhu, Lewei Lu, et al. Internvl: Scaling up vision foundation models and aligning for generic visual-linguistic tasks. In *Proceedings of the IEEE/CVF Conference on Computer Vision and Pattern Recognition*, pp. 24185–24198, 2024b.
- Cody Coleman, Christopher Yeh, Stephen Mussmann, Baharan Mirzasoleiman, Peter Bailis, Percy Liang, Jure Leskovec, and Matei Zaharia. Selection via proxy: Efficient data selection for deep learning. In *International Conference on Learning Representations*, 2019.
- Jacob Devlin, Ming-Wei Chang, Kenton Lee, and Kristina Toutanova. Bert: Pre-training of deep bidirectional transformers for language understanding, 2019. URL <https://arxiv.org/abs/1810.04805>.
- Zhang Ge, Du Xinrun, Chen Bei, Liang Yiming, Luo Tongxu, Zheng Tianyu, Zhu Kang, Cheng Yuyang, Xu Chunpu, Guo Shuyue, Zhang Haoran, Qu Xingwei, Wang Junjie, Yuan Ruibin, Li Yizhi, Wang Zekun, Liu Yudong, Tsai Yu-Hsuan, Zhang Fengji, Lin Chenghua, Huang Wenhao, and Fu Jie. Cmmu: A chinese massive multi-discipline multimodal understanding benchmark. *GitHub repository*, 2024.
- Yash Goyal, Tejas Khot, Douglas Summers-Stay, Dhruv Batra, and Devi Parikh. Making the V in VQA matter: Elevating the role of image understanding in Visual Question Answering. In *Conference on Computer Vision and Pattern Recognition (CVPR)*, 2017.
- Danna Gurari, Qing Li, Abigale J Stangl, Anhong Guo, Chi Lin, Kristen Grauman, Jiebo Luo, and Jeffrey P Bigham. Vizwiz grand challenge: Answering visual questions from blind people. In *Proceedings of the IEEE conference on computer vision and pattern recognition*, pp. 3608–3617, 2018.
- Jack Hessel, Ari Holtzman, Maxwell Forbes, Ronan Le Bras, and Yejin Choi. Clipscore: A reference-free evaluation metric for image captioning, 2022. URL <https://arxiv.org/abs/2104.08718>.
- Edward J Hu, Yelong Shen, Phillip Wallis, Zeyuan Allen-Zhu, Yanzhi Li, Shean Wang, Lu Wang, and Weizhu Chen. Lora: Low-rank adaptation of large language models. *arXiv preprint arXiv:2106.09685*, 2021.
- Drew A Hudson and Christopher D Manning. Gqa: A new dataset for real-world visual reasoning and compositional question answering. In *Proceedings of the IEEE/CVF conference on computer vision and pattern recognition*, pp. 6700–6709, 2019.
- Aniruddha Kembhavi, Mike Salvato, Eric Kolve, Minjoon Seo, Hannaneh Hajishirzi, and Ali Farhadi. A diagram is worth a dozen images. In *Computer Vision—ECCV 2016: 14th European Conference, Amsterdam, The Netherlands, October 11–14, 2016, Proceedings, Part IV 14*, pp. 235–251. Springer, 2016.



- Zaid Khan, Elias Stengel-Eskin, Jaemin Cho, and Mohit Bansal. Dataenvgym: Data generation agents in teacher environments with student feedback. In *The Thirteenth International Conference on Learning Representations*, 2025.
- M Kumar, Benjamin Packer, and Daphne Koller. Self-paced learning for latent variable models. *Advances in neural information processing systems*, 23, 2010.
- Jaewoo Lee, Boyang Li, and Sung Ju Hwang. Concept-skill transferability-based data selection for large vision-language models. In *Proceedings of the 2024 Conference on Empirical Methods in Natural Language Processing*, pp. 5060–5080, 2024.
- Bohao Li, Rui Wang, Guangzhi Wang, Yuying Ge, Yixiao Ge, and Ying Shan. Seed-bench: Benchmarking multimodal llms with generative comprehension. *arXiv preprint arXiv:2307.16125*, 2023a.
- Yifan Li, Yifan Du, Kun Zhou, Jinpeng Wang, Wayne Xin Zhao, and Ji-Rong Wen. Evaluating object hallucination in large vision-language models. In *The 2023 Conference on Empirical Methods in Natural Language Processing*, 2023b. URL <https://openreview.net/forum?id=xozJw0kZXF>.
- Zijing Liang, Yanjie Xu, Yifan Hong, Penghui Shang, Qi Wang, Qiang Fu, and Ke Liu. A survey of multimodal large language models. In *Proceedings of the 3rd International Conference on Computer, Artificial Intelligence and Control Engineering*, pp. 405–409, 2024.
- Haotian Liu, Chunyuan Li, Yuheng Li, and Yong Jae Lee. Improved baselines with visual instruction tuning. *arXiv preprint arXiv:2310.03744*, 2023a.
- Haotian Liu, Chunyuan Li, Qingyang Wu, and Yong Jae Lee. Visual instruction tuning. In *Advances in Neural Information Processing Systems (NeurIPS)*, 2023b.
- Yuan Liu, Haodong Duan, Yuanhan Zhang, Bo Li, Songyang Zhang, Wangbo Zhao, Yike Yuan, Jiaqi Wang, Conghui He, Ziwei Liu, et al. Mmbench: Is your multi-modal model an all-around player? In *European conference on computer vision*, pp. 216–233. Springer, 2024a.
- Zikang Liu, Kun Zhou, Wayne Xin Zhao, Dawei Gao, Yaliang Li, and Ji-Rong Wen. Less is more: High-value data selection for visual instruction tuning, 2024b. URL <https://arxiv.org/abs/2403.09559>.
- Pan Lu, Swaroop Mishra, Tanglin Xia, Liang Qiu, Kai-Wei Chang, Song-Chun Zhu, Oyvind Tafjord, Peter Clark, and Ashwin Kalyan. Learn to explain: Multimodal reasoning via thought chains for science question answering. *Advances in Neural Information Processing Systems*, 35:2507–2521, 2022.
- Adyasha Maharana, Prateek Yadav, and Mohit Bansal. D2 pruning: Message passing for balancing diversity and difficulty in data pruning. In *Proceedings of the International Conference on Learning Representations (ICLR)*, 2024.
- Adyasha Maharana, Jaehong Yoon, Tianlong Chen, and Mohit Bansal. Adapt- $\infty$ : Scalable continual multimodal instruction tuning via dynamic data selection, 2025. URL <https://arxiv.org/abs/2410.10636>.
- Max Marion, Ahmet Üstün, Luiza Pozzobon, Alex Wang, Marzieh Fadaee, and Sara Hooker. When less is more: Investigating data pruning for pretraining llms at scale. *arXiv preprint arXiv:2309.04564*, 2023.
- Ahmed Masry, Xuan Long Do, Jia Qing Tan, Shafiq Joty, and Enamul Hoque. Chartqa: A benchmark for question answering about charts with visual and logical reasoning. In *Findings of the Association for Computational Linguistics: ACL 2022*, pp. 2263–2279, 2022.
- Sören Mindermann, Jan M Brauner, Muhammed T Razzak, Mrinank Sharma, Andreas Kirsch, Winnie Xu, Benedikt Höltingen, Aidan N Gomez, Adrien Morisot, Sebastian Farquhar, et al. Prioritized training on points that are learnable, worth learning, and not yet learnt. In *International Conference on Machine Learning*, pp. 15630–15649. PMLR, 2022.

- Ishan Misra, Ross Girshick, Rob Fergus, Martial Hebert, Abhinav Gupta, and Laurens van der Maaten. Learning by asking questions, 2017. URL <https://arxiv.org/abs/1712.01238>.
- OpenAI, Josh Achiam, and et al. Gpt-4 technical report, 2024. URL <https://arxiv.org/abs/2303.08774>.
- Maxime Oquab, Timothée Darcet, Théo Moutakanni, Huy Vo, Marc Szafraniec, Vasil Khalidov, Pierre Fernandez, Daniel Haziza, Francisco Massa, Alaaeldin El-Nouby, Mahmoud Assran, Nicolas Ballas, Wojciech Galuba, Russell Howes, Po-Yao Huang, Shang-Wen Li, Ishan Misra, Michael Rabbat, Vasu Sharma, Gabriel Synnaeve, Hu Xu, Hervé Jegou, Julien Mairal, Patrick Labatut, Armand Joulin, and Piotr Bojanowski. Dinov2: Learning robust visual features without supervision, 2024. URL <https://arxiv.org/abs/2304.07193>.
- Mansheej Paul, Surya Ganguli, and Gintare Karolina Dziugaite. Deep learning on a data diet: Finding important examples early in training. *Advances in neural information processing systems*, 34: 20596–20607, 2021.
- Alec Radford, Jong Wook Kim, Chris Hallacy, Aditya Ramesh, Gabriel Goh, Sandhini Agarwal, Girish Sastry, Amanda Askell, Pamela Mishkin, Jack Clark, et al. Learning transferable visual models from natural language supervision. In *Proceedings of the International Conference on Machine Learning (ICML)*, 2021.
- Mrimmaya Sachan and Eric Xing. Easy questions first? a case study on curriculum learning for question answering. In *Proceedings of the 54th Annual Meeting of the Association for Computational Linguistics (Volume 1: Long Papers)*, pp. 453–463, 2016.
- Amanpreet Singh, Vivek Natarajan, Meet Shah, Yu Jiang, Xinlei Chen, Dhruv Batra, Devi Parikh, and Marcus Rohrbach. Towards vqa models that can read. In *Proceedings of the IEEE/CVF conference on computer vision and pattern recognition*, pp. 8317–8326, 2019.
- Ben Sorscher, Robert Geirhos, Shashank Shekhar, Surya Ganguli, and Ari Morcos. Beyond neural scaling laws: beating power law scaling via data pruning. *Advances in Neural Information Processing Systems*, 35:19523–19536, 2022.
- Gemini Team, Rohan Anil, Sebastian Borgeaud, Yonghui Wu, Jean-Baptiste Alayrac, Jiahui Yu, Radu Soricut, Johan Schalkwyk, Andrew M Dai, Anja Hauth, et al. Gemini: a family of highly capable multimodal models. *arXiv preprint arXiv:2312.11805*, 2023.
- Lev S Vygotsky. *Thought and language*, volume 29. MIT press, 2012.
- Peng Wang, Shuai Bai, Sinan Tan, Shijie Wang, Zhihao Fan, Jinze Bai, Keqin Chen, Xuejing Liu, Jialin Wang, Wenbin Ge, Yang Fan, Kai Dang, Mengfei Du, Xuancheng Ren, Rui Men, Dayiheng Liu, Chang Zhou, Jingren Zhou, and Junyang Lin. Qwen2-vl: Enhancing vision-language model’s perception of the world at any resolution. *arXiv preprint arXiv:2409.12191*, 2024.
- Xindi Wu, Mengzhou Xia, Rulin Shao, Zhiwei Deng, Pang Wei Koh, and Olga Russakovsky. Icons: Influence consensus for vision-language data selection, 2025. URL <https://arxiv.org/abs/2501.00654>.
- Mengzhou Xia, Sadhika Malladi, Suchin Gururangan, Sanjeev Arora, and Danqi Chen. Less: Selecting influential data for targeted instruction tuning. In *Forty-first International Conference on Machine Learning*, 2024.
- Zhiyang Xu, Chao Feng, Rulin Shao, Trevor Ashby, Ying Shen, Di Jin, Yu Cheng, Qifan Wang, and Lifu Huang. Vision-flan: Scaling human-labeled tasks in visual instruction tuning. *arXiv preprint arXiv:2402.11690*, 2024.
- Yanzhe Zhang, Ruiyi Zhang, Jiuxiang Gu, Yufan Zhou, Nedim Lipka, Diyi Yang, and Tong Sun. Llavav: Enhanced visual instruction tuning for text-rich image understanding. *arXiv preprint arXiv:2306.17107*, 2023.
- Baichuan Zhou, Ying Hu, Xi Weng, Junlong Jia, Jie Luo, Xien Liu, Ji Wu, and Lei Huang. Tinyllava: A framework of small-scale large multimodal models. *arXiv preprint arXiv:2402.14289*, 2024.